Hindawi
International Journal of Photoenergy
Volume 2022, Article ID 3604240, 6 pages
https://doi.org/10.1155/2022/3604240

Research Article

Performance Enhancement of Hybrid Energy Devices Using Cooling Patches

Jaehwan Lee,[1] **Kyoungah Cho**,[1] **Yoonbeom Park**,[1] **Sungeun Park**,[2] **Hee-eun Song**,[2] **and Sangsig Kim**[1]

[1]*Department of Electrical Engineering, Korea University, Seoul 02841, Republic of Korea*
[2]*Photovoltaic Laboratory, Korea Institute of Energy Research, Daejeon 34129, Republic of Korea*

Correspondence should be addressed to Kyoungah Cho; chochem@korea.ac.kr and Sangsig Kim; sangsig@korea.ac.kr

Received 2 March 2022; Accepted 21 September 2022; Published 6 October 2022

Academic Editor: Zaiyong Jiang

In this study, we demonstrated the enhancement of the output power of a hybrid energy device (HED) using a cooling patch that does not consume any external electric power. The HED consisted of a photovoltaic cell (PVC) and a thermoelectric generator (TEG); the cooling patch was attached to the TEG. When the PVC was exposed to solar irradiance, the cooling patch lowered the temperature of the PVC and increased the thermal gradient across the TEG, thereby increasing the output power. For an HED with a cooling patch at an irradiance of 1000 W/m^2, the output power increased to 24.2 mW, as compared to the output power of 19.9 mW for an HED without any cooling patch.

1. Introduction

Recently, hybrid energy devices (HEDs) consisting of photovoltaic cells (PVCs) and thermoelectric generators (TEGs) have emerged as novel renewable energy devices to maximize the conversion of solar energy into electricity [1–3]. Although solar energy has been used in a wide range of fields [4–8], it still plays a leading role as renewable energy sources. When a PVC is exposed to solar irradiance, it produces electrical energy and its temperature increases; the thermal energy corresponding to the increased temperature is converted into electrical energy via a TEG. The PVC and TEG are electrically connected to each other in an HED; therefore, the output power of an HED is the summation of the electrical energies produced by both the PVC and TEG. The energy efficiency of a PVC is higher than that of a TEG; thus, the output power of an HED mainly depends on the performance of the PVC [9–11].

The temperature increased by solar irradiance degrades the efficiency of the PVC [12, 13], whereas the corresponding thermal energy is responsible for the thermal gradients across the TEG leading to the generation of Seebeck voltages. To increase the output power of an HED, the temperature of the PVC should be lowered, and the thermal gradients across the TEG should be larger. Recently, highly conductive thermal interfaces and electrical cooling systems have been researched to increase the thermal gradients; such interfaces between PVCs and TEGs increase the temperatures of hot electrodes in TEGs [9, 10], while electrical cooling systems decrease the temperatures of the cold electrodes in TEGs [11–13]. Nevertheless, no significant research has been conducted pertaining to the lowering of PVC temperatures and the enhancement of the output power in HEDs using highly conductive thermal interfaces and cooling systems. Moreover, the electrical cooling systems used in recent studies consume electrical energy [16–18]; therefore, new cooling systems operating without external power should be utilized in HEDs.

In this study, we prepared a mixture of hexagonal boron nitride (h-BN) and carbon paste to make a highly conductive thermal interface. An HED consisting of a PVC and TEG with a mixture of h-BN and carbon paste present between them was utilized, and a cooling patch that did not require the external power was attached to the TEG. The cooling patch contains a superabsorbent polymer being a heat absorbent material so that it can lower the temperature by absorbing the heat transferred to the TEG from the PVC. We thus

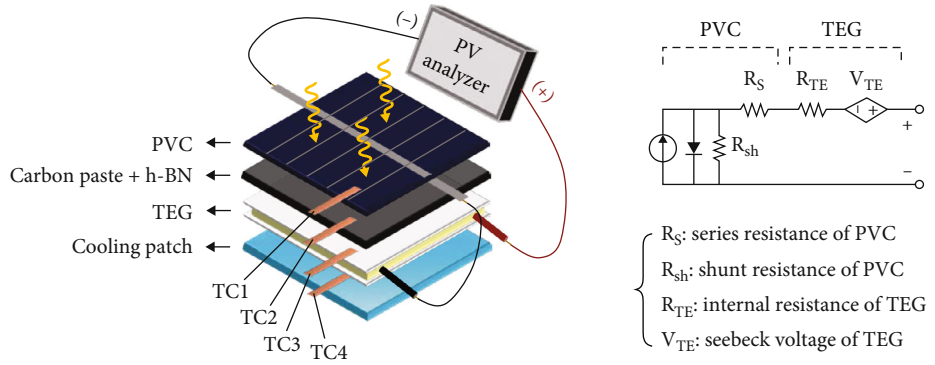

Figure 1: Schematic and circuit diagrams of a HED with a cooling patch.

examined the temperature lowering of the PVC and the output power enhancement of the HED using the cooling patch.

2. Materials and Methods

The schematic and circuit diagram of the HED constructed using a c-Si PVC, an interface material layer, and a TEG are depicted in Figure 1; the dimensions of the HED were 2.0 cm (width) × 2.0 cm (length) × 5.2 mm (height; the sum of the thicknesses of the PVC (0.2 mm), interface (1.0 mm), and TEG (4.0 mm)). The c-Si PVC was fabricated as described in the previous studies [19, 20]; its series resistance (R_s) and shunt resistance (R_{sh}) were 0.8 and 500 Ω, respectively. The TEG with a R_{TE} of 1 Ω and a Seebeck coefficient of 7.7 mV/K was purchased from Peltier Testing System Co. Ltd. The interface material layer between the PVC and TEG was made by mixing the h-BN (purchased from 3 M) and carbon paste (purchased from Dycotec Materials Ltd.) with a weight ratio of 1 : 10; its thermal conductivity was estimated to be approximately 315.4 W/m•K based on its thermal diffusivity [21]. The mixing ratio of h-BN and carbon paste was optimized for good adhesion between the PVC and TEG; the adhesion is responsible for the stability of the HED in terms of the structure. The cooling patch purchased from Kokubo and Co. Ltd. was attached to the cold electrode of the TEG. The temperatures of the HED were measured at four positions with type K thermocouples (TCs); TC1 and TC2 were attached to the top and bottom sides of the PVC, respectively, and TC3 and TC4 were attached to the top (hot electrode) and bottom (cold electrode) of the TEG, respectively.

The experimental setup and optical image of the HED are shown in Figure 2. The electrical characteristics of the HED were examined with a PV analyzer (PROVA-200A). A solar simulator (XG-100E, Xelios) was used as the solar energy source, and the irradiance was measured using a pyranometer (MS-40, EKO Instruments Co., Ltd.).

3. Results and Discussion

The temperatures of the HEDs (a) without and (b) with the cooling patch are plotted as a function of irradiance in Figure 3. $T1$ and $T2$ denote the temperatures of the top and bottom of the PVC, respectively, and $T3$ and $T4$ denote the temperatures of the top and bottom of the TEG, respectively. The temperatures of the HED with the cooling patch were observed to be lower than those of the HED without the cooling patch. The cooling patch not only lowered the PVC temperatures $T1$ and $T2$ but also increased the difference between $T3$ and $T4$, i.e., the TEG electrode temperatures (thermal gradient increased across the TEG). In particular, at a solar irradiance of 1000 W/m^2, in the presence of the cooling patch, the PVC temperatures $T1$ and $T2$ were lowered by 9°C and the difference between the TEG temperatures $T3$ and $T4$ was twice as large as that in the absence of the cooling patch.

The current-voltage (I-V) curves of the HEDs are plotted in Figure 4 in the (a) absence and (b) presence of the cooling patch at irradiances in the range of 200 to 1000 W/m^2. The short-circuit current (I_{sc}) increased from 14 to 101 mA as the irradiance increased from 200 to 1000 W/m^2 for both the HEDs with and without the cooling patch. In contrast, for the HED with the cooling patch, the open-circuit voltage (V_{OC}) increased with the increase in solar irradiance; at a solar irradiance of 1000 W/m^2, the V_{OC} increased from 0.59 to 0.65 V. The increase in V_{OC} implies a shift toward the higher voltage region caused by the Seebeck voltage generated by the TEG [22]. The cooling patch contributes to the increase in the thermal gradient across the TEG, i.e., the increase in the difference between $T3$ and $T4$ temperatures, thereby enhancing the Seebeck voltage.

The output power of the HED is the summation of the output powers of the PVC and TEG; the PVC acts as the primary power source, and the TEG acts as an auxiliary power source [23–25]. The energy efficiency of the PVC, which is three times larger than that of the TEG, reduces with the increasing temperature [12, 13], which in turn significantly decreases the output power of the HED. The rate of increase in the PVC temperature caused by the increasing solar irradiance is lowered by the cooling patch, which contributes to the enhancement of the maximum output power (P_{max}) of the HED. Figure 5 shows the output power curves of the HEDs with and without the cooling patch at irradiances of (a) 200 W/m^2 to (e) 1000 W/m^2 and (f) the increment in

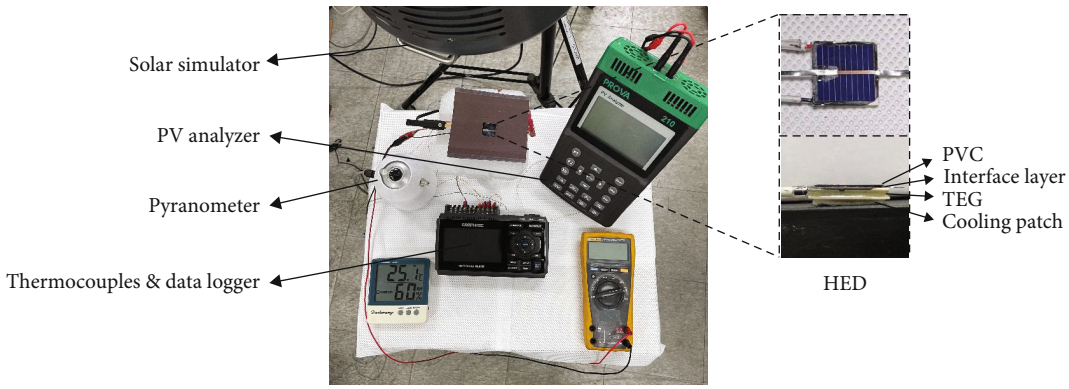

Figure 2: Experimental set-up and the optical image of the HED.

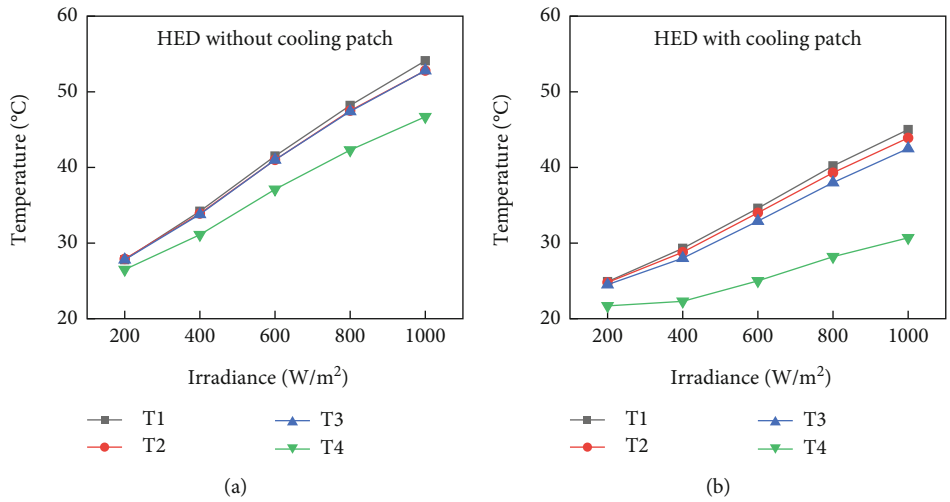

Figure 3: Temperatures of HEDs (a) without and (b) with the cooling patch at irradiances in the range of 200 to 1000 W/m^2.

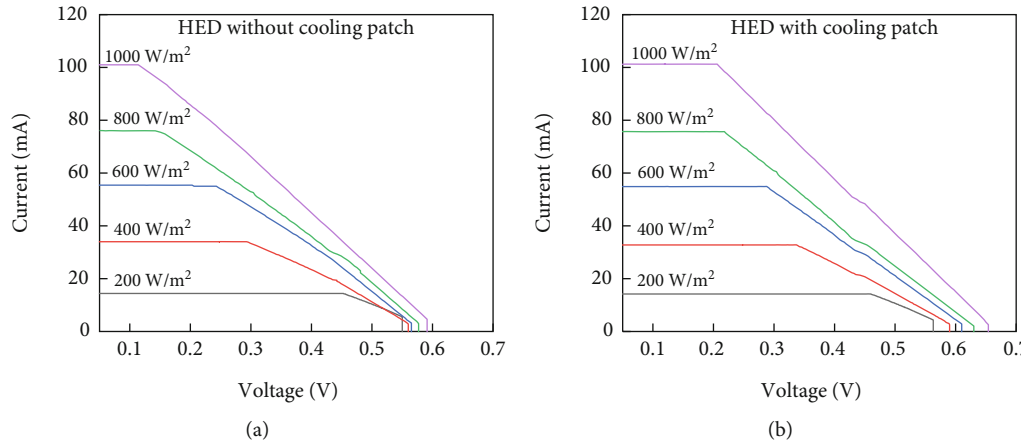

Figure 4: The I-V curves of the HEDs (a) without cooling patch and (b) with cooling patch.

P_{max} owing to the cooling patch. P_{max} increases up to over 21% (from 19.9 to 24.2 mW) at the irradiance of 1000 W/m^2 after applying the cooling patch, although the cooling patch was less effective at the irradiance of 200 W/m^2. The increase in the P_{max} of the HED with the cooling patch is attributed to the lowering of the temperature of the entire HED consisting of the PVC and TEG as shown in Figure 3. Considering that the output power of the PVC is reduced by 0.5 ~ 1% as the temperature is increased by 1°C [12, 13], the lowering of the temperature of the PVC is

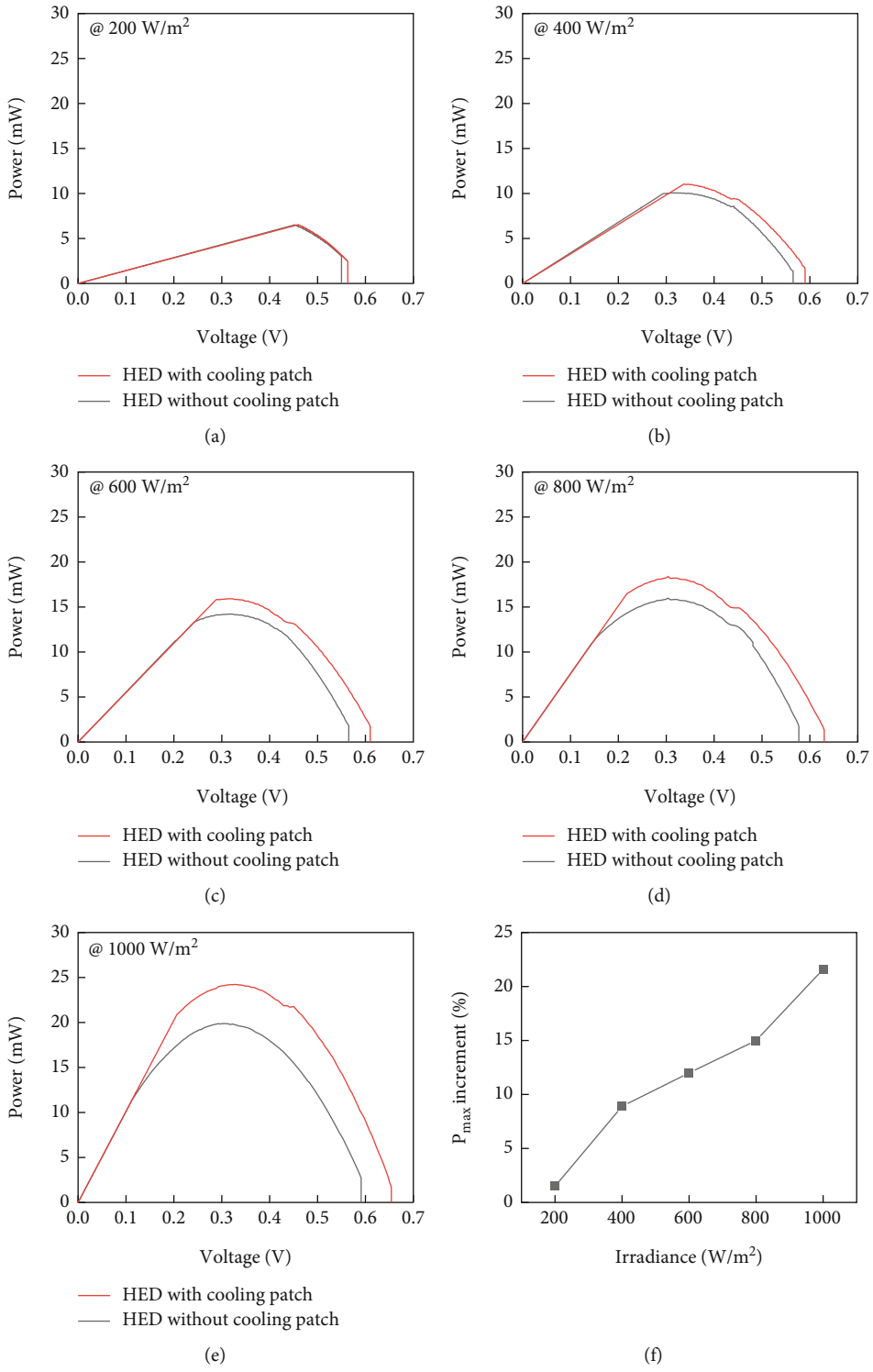

Figure 5: The output power curves of HEDs without and with the cooling patch at different irradiance levels: (a) 200 W/m^2, (b) 400 W/m^2, (c) 600 W/m^2, (d) 800 W/m^2, (e) 1000 W/m^2, and (f) P_{max} increment of the HEDs with the cooling patch at irradiances in the range of 200 to 1000 W/m^2.

deeply concerned with the enhancement in output power of the PVC. Moreover, the cooling patch attached to the bottom side of the TEG makes large temperature difference between $T3$ and $T4$ so that it contributes significantly to the output power generated by the TEG. The enhancement in the individual output power of the PVC and TEG results in the increase in the P_{max} of the HED because the output power of the HED is the summation of the output powers of the PVC and TEG. This study demonstrates the improvement in the output power of the HED using a cooling patch.

4. Conclusions

In this study, we proposed a method to enhance the output power of the HED by using a cooling patch on the cold electrode of a TEG and investigated the relationship between the temperature of the PVC and the output power of the HED. For solar irradiances from 200 to 1000 W/m^2, the cooling patch reduced the entire temperature of the HED. The reduction in the PVC temperature and the increase in the thermal gradient across the TEG by the cooling patch substantially contributed to the enhancement of the output power of the HED. At the irradiance of 1000 W/m^2, the increment in the maximum output power reached over 21% owing to the utilization of the cooling patch that did not consume any external power.

Data Availability

The data used to support the findings of this study are included within the article.

Conflicts of Interest

The authors declare that there is no conflict of interest regarding the publication of this paper.

Acknowledgments

This study was supported by the Technology Development Program to Solve Climate Changes (NRF-2017M1A2A2087323), the National Research Foundation of Korea (NRF) grant funded by the Korean government (MSIT) (NRF-2020R1A2C3004538, NRF-2022M3I7A3046571), the Brain Korea 21 Plus Project in 2022 through the NRF funded by the Ministry of Science, and the Korea University Grant.

References

[1] Y. Li, S. Witharana, H. Cao, M. Lasfargues, Y. Huang, and Y. Ding, "Wide spectrum solar energy harvesting through an integrated photovoltaic and thermoelectric system," *Particuology*, vol. 15, pp. 39–44, 2014.

[2] Y. Deng, W. Zhu, Y. Wang, and Y. Shi, "Enhanced performance of solar-driven photovoltaic-thermoelectric hybrid system in an integrated design," *Solar Energy*, vol. 88, pp. 182–191, 2013.

[3] X. Ju, Z. Wang, G. Flamant, P. Li, and W. Zhao, "Numerical analysis and optimization of a spectrum splitting concentration photovoltaic-thermoelectric hybrid system," *Solar Energy*, vol. 86, no. 6, pp. 1941–1954, 2012.

[4] S. Li, M. Cai, C. Wang et al., "Rationally designed Ta_3N_5/BiOCl S-scheme heterojunction with oxygen vacancies for elimination of tetracycline antibiotic and Cr(VI): Performance, toxicity evaluation and mechanism insight," *Journal of Materials Science & Technology*, vol. 123, pp. 177–190, 2022.

[5] S. Li, M. Cai, Y. Liu, C. Wang, R. Yan, and X. Chen, "Constructing $Cd_{0.5}Zn_{0.5}S/Bi_2WO_6$ S-scheme heterojunction for boosted photocatalytic antibiotic oxidation and Cr(VI) reduction," *Advanced Powder Materials*, vol. 2, no. 1, article 100073, 2023.

[6] S. Li, C. Wang, Y. Liu et al., "Photocatalytic degradation of tetracycline antibiotic by a novel $Bi_2Sn_2O_7/Bi_2MoO_6$ S-scheme heterojunction: performance, mechanism insight and toxicity assessment," *Chemical Engineering Journal*, vol. 429, p. 132519, 2022.

[7] S. Li, M. Cai, Y. Liu et al., "*In situ* construction of a C_3N_5 nanosheet/Bi_2WO_6 nanodot S-scheme heterojunction with enhanced structural defects for the efficient photocatalytic removal of tetracycline and Cr(vi)," *Inorganic Chemistry Frontiers*, vol. 9, no. 11, pp. 2479–2497, 2022.

[8] C. Wang, S. Li, M. Cai et al., "Rationally designed tetra (4-carboxyphenyl) porphyrin/graphene quantum dots/bismuth molybdate Z-scheme heterojunction for tetracycline degradation and Cr(VI) reduction: Performance, mechanism, intermediate toxicity appraisement," *Journal of Colloid and Interface Science*, vol. 619, pp. 307–321, 2022.

[9] K. Yoshikawa, H. Kawasaki, W. Yoshida et al., "Silicon heterojunction solar cell with interdigitated back contacts for a photoconversion efficiency over 26%," *Nature Energy*, vol. 2, no. 5, article 17032, 2017.

[10] D. Kraemer, Q. Jie, K. McEnaney et al., "Concentrating solar thermoelectric generators with a peak efficiency of 7.4%," *Nature Energy*, vol. 1, no. 11, article 16153, 2016.

[11] F. Haase, C. Hollemann, S. Schäfer et al., "Laser contact openings for local poly-Si-metal contacts enabling 26.1%-efficient POLO-IBC solar cells," *Solar Energy Materials and Solar Cells*, vol. 186, pp. 184–193, 2018.

[12] V. J. Fesharaki, M. Dehghani, J. J. Fesharaki, and H. Tavasoli, "The effect of temperature on photovoltaic cell efficiency," in *Proceedings of the 1st International Conference on Emerging Trends in Energy Conservation–ETEC*, Tehran, Iran, 2011.

[13] P. Singh and N. M. Ravindra, "Temperature dependence of solar cell performance–an analysis," *Solar Energy Materials and Solar Cells*, vol. 101, pp. 36–45, 2012.

[14] J. Zhang, H. Zhai, Z. Wu, Y. Wang, H. Xie, and M. Zhang, "Enhanced performance of photovoltaic-thermoelectric coupling devices with thermal interface materials," *Energy Reports*, vol. 6, pp. 116–122, 2020.

[15] E. Yin, Q. Li, and Y. Xuan, "Thermal resistance analysis and optimization of photovoltaic-thermoelectric hybrid system," *Energy Conversion and Management*, vol. 143, pp. 188–202, 2017.

[16] S. Soltani, A. Kasaeian, H. Sarrafha, and D. Wen, "An experimental investigation of a hybrid photovoltaic/thermoelectric system with nanofluid application," *Solar Energy*, vol. 155, pp. 1033–1043, 2017.

[17] J. Zhang, Y. Xuan, and L. Yang, "Performance estimation of photovoltaic-thermoelectric hybrid systems," *Energy*, vol. 78, pp. 895–903, 2014.

[18] W. Gu, T. Ma, A. Song, M. Li, and L. Shen, "Mathematical modelling and performance evaluation of a hybrid photovoltaic- thermoelectric system," *Energy Conversion and Management*, vol. 198, p. 111800, 2019.

[19] J. Kim, J. Park, J. H. Hong et al., "Double antireflection coating layer with silicon nitride and silicon oxide for crystalline silicon solar cell," *Journal of Electroceramics*, vol. 30, no. 1-2, pp. 41–45, 2013.

[20] J.-K. Lee, J.-S. Lee, Y.-S. Ahn et al., "Photovoltaic performance of c-Si wafer reclaimed from end-of-life solar cell using various mixing ratios of HF and HNO_3," *Solar Energy Materials and Solar Cells*, vol. 160, pp. 301–306, 2017.

[21] Y. Park, K. Cho, and S. Kim, "Performance prediction of hybrid energy harvesting devices using machine learning," *ACS Applied Materials & Interfaces*, vol. 14, no. 9, pp. 11248–11254, 2022.

[22] Y. Park, K. Cho, S. Yang et al., "Performance of hybrid energy devices consisting of photovoltaic cells and thermoelectric generators," *ACS Applied Materials & Interfaces*, vol. 12, no. 7, pp. 8124–8129, 2020.

[23] K.-T. Park, S. M. Shin, A. S. Tazebay et al., "Lossless hybridization between photovoltaic and thermoelectric devices," *Scientific Reports*, vol. 3, no. 1, article 2123, 2013.

[24] J. Zhang and Y. Xuan, "The electric feature synergy in the photovoltaic - thermoelectric hybrid system," *Energy*, vol. 181, pp. 387–394, 2019.

[25] Y. Park, K. Cho, S. Yang et al., "Effect of net voltage of thermoelectric generator on performance of hybrid energy device," *Energy Reports*, vol. 6, pp. 2836–2840, 2020.